Nancy S. Pollard

Robotics Institute, Carnegie Mellon University
Pittsburgh, PA 15213-3890, USA
ATR Computational Neuroscience Laboratories
Kyoto, Japan
nsp@cs.cmu.edu

Closure and Quality Equivalence for Efficient Synthesis of Grasps from Examples

Abstract

One goal of grasp selection for robotics is to choose contact points that guarantee properties such as force- or form-closure. Many efficient algorithms have been developed to address this problem, but most of these algorithms focus on grasps having a minimal number of contact points. Increasing the number of contacts can dramatically improve the quality and flexibility of grasps that are constructed. However, computation time becomes a problem, as grasp synthesis algorithms that can be generalized to an arbitrary number of contacts typically require time exponential in the number of contacts. This paper presents an efficient algorithm for synthesis of many-contact grasps. The key idea is to geometrically construct families of grasps around a single example such that all grasps within a family meet user-specified design goals. We show that our construction technique can be used to form force-closure grasps, partial force-closure grasps, and grasps above a quality threshold. Our approach requires time polynomial in the number of contacts, making it feasible to handle grasps with relatively large numbers of contacts. Results are shown for three-dimensional grasps with friction having five to twelve contacts and specialized for a variety of tasks. We have used this approach to design grasps for a robot hand and quasi-static manipulation plans for a humanoid robot.

KEY WORDS—grasping, grasp synthesis, example-based grasping, enveloping grasps, grasp quality, contact regions

1. Nomenclature

Problem size

N = number of contacts in a grasp
L = number of unit wrenches used in a contact model
H = number of half-spaces bounding a convex hull

Indices

n = index used for contacts
l = index used for wrenches in a contact model
h = index used for half-spaces

Contact wrenches (Section 4)

$\hat{\mathbf{w}}_l(c)$ = a unit wrench available at contact c, normalized for unit force normal to the surface
$Y(c) = 6xL$ matrix containing unit wrenches $\hat{\mathbf{w}}_l(c)$
$\alpha = Lx1$ vector of coefficients; $Y(c)\alpha$ is a valid unit wrench at c if $\alpha \geq \mathbf{0}$ and $||\alpha||_{L_1} = 1$

Grasps and grasp families (Sections 5–7)

g_n = contact n of an example grasp
G = example grasp, the set of unit wrenches available at all contacts: $G = \{\hat{\mathbf{w}}_1(g_1), \ldots, \hat{\mathbf{w}}_L(g_N)\}$
$CH_{orig}(G)$ = the convex hull of wrenches in G: $ConvexHull\{\hat{\mathbf{w}}_1(g_1), \ldots, \hat{\mathbf{w}}_L(g_N)\}$
$\hat{\mathbf{n}}_h$ = half-space normal h, normalized using the L_2 norm in $\mathbb{R}^6$
d_h = distance from the origin of half-space h in direction $\hat{\mathbf{n}}_h$
ϵ_h = replaces d_h to create half-spaces tailored to a given task (Sections 5–7)
ϵ = vector containing all ϵ_h values: $\epsilon = [\epsilon_1 \ldots \epsilon_H]^{\mathrm{T}}$, determined by the task (Section 7)
$W(G, \epsilon)$ = set of grasps "similar" to G given ϵ, defined as $\{c_1, \ldots, c_N : c_n \in W_n(G, \epsilon), n = 1, \ldots, N\}$
$W_n(G, \epsilon)$ = set of all contacts "similar" to contact g_n given ϵ, defined as $\bigcap_{l=1}^{L} W_{n,l}(G, \epsilon)$
$W_{n,l}(G, \epsilon)$ = set of all contacts "similar" to contact g_n when a single wrench $\hat{\mathbf{w}}_l(g_n)$ is considered
$CH_{new}(C)$ = convex hull of unit wrenches in new grasp: $C \in W(G, \epsilon) \longrightarrow CH_{new}(C) \supseteq CH_{eps}(G, \epsilon)$ (Section 6)
$CH_{eps}(G, \epsilon)$ = volume contained by the convex hull of unit wrenches of any grasp in $W(G, \epsilon)$ (Section 6)

The International Journal of Robotics Research
Vol. 23, No. 6, June 2004, pp. 595-613,
DOI: 10.1177/0278364904044402

β = minimum quality of a new grasp expressed relative to the example; determines ϵ_h (Section 7)

Contact targets (Section 8)

$P_j([\hat{\mathbf{n}}_h d_h]^{\mathrm{T}})$ = exterior of half-space boundary h projected onto a given plane

$P(W_n)$ = contact region W_n projected onto a given plane

$P_{j,3D}([\hat{\mathbf{n}}_h d_h]^{\mathrm{T}})$ = exterior of half-space boundary h projected into 3D Cartesian space, given an expected normal

$P_{3D}(W_n)$ = contact region W_n projected into 3D Cartesian space, given an expected normal

2. Introduction

For many human grasps, the hand conforms closely to the object surface (Figure 1). The fingers may wrap around the handle of a hammer, wrench, or other tool, contact the sides and bottom of a heavy mug, or provide support along the bottom of a basket or bowl. Synthesizing grasps similar to these real-world examples requires considering large areas of contact between the hand and object or, as an approximation, a large number of point contacts. Even in more traditional robotics settings, having a large number of contacts may be useful. In fixture design, for example, additional contacts may provide flexibility in contact placement when feasible contact areas are highly constrained.

Synthesis of grasps having large numbers of contacts remains a challenge, however. When the goal is to produce an optimal grasp, fast constructive solutions are not yet available for grasps having more than four contacts. Global optimization requires time exponential in the number of contacts and becomes increasingly impractical as the number of contacts grows. Local optimization may have problems with local minima and relies on a good initial guess.

This paper explores an alternative to grasp optimization. Instead of providing a function that should be optimized, we provide a single example of a successful grasp and synthesize only grasps that preserve properties of that example. Properties that can be preserved easily using our approach include force-closure, partial force-closure, and force-based quality measures such as those described by Kirkpatrick, Mishra, and Yap (1990), Li and Sastry (1987), and Zhu, Ding, and Li (2001). We use these quality measures to quantify the goal that a new grasp be "almost as good as the example", and show how families of grasps can be constructed to meet this goal.

Figures 2 and 3 show some of our results. In Figure 2, the left column shows an example grasp composed of eight hard-finger contacts with friction. Our algorithm, outlined in Figure 4, constructs a family of grasps from the example and can project these results onto any object geometry to form target contact regions as shown. The role of the example grasp is to determine the locations of the contact regions. To illustrate the effect of changing the example grasp, Figure 3 shows results for a four-contact grasp as the example moves up the side of the object. The families of grasps shown in Figures 2 and 3 preserve the property that grasps within each family must be at least 90% as good as the example for supporting the object against gravity, using the quality metric of Zhu, Ding, and Li (2001). The absolute quality of the results depends on the quality of the example. Quality guaranteed for grasps in Figure 3(C), for instance, is only 53% as high as that guaranteed for grasps in Figure 3(A). However, if the user has provided the example in Figure 3(C) because he wishes the robot to grasp near the top of the basket, then the grasps constructed around this example may in practice be very good solutions.

The idea of creating grasp families is not new (e.g., Nguyen 1988; Ponce et al. 1997), and computation of contact regions is useful for accommodating errors and constraints in contact placement. For example, the problem of placing two hands to achieve eight contact points on an object is very highly constrained, and having large target regions such as those shown in Figure 2 can help make it possible to meet those constraints. However, existing techniques for computing contact regions require time exponential in the number of contacts and have not been presented for a number of contacts larger than four. By constructing a family of grasps around an example, we are able to construct contact regions in time polynomial in the number of contacts, making this idea more practical for many-contact grasps.

Preliminary versions of this work appeared in Pollard (1996) and Pollard and Hodgins (2002). The major theoretical contribution of the current paper is to quantify the results of our construction technique (Section 6); we can now state precisely what properties of the example grasp are preserved in our approach and use this result to tailor grasp families to a specific task. The major practical contributions are to present an extension to partial force-closure (Section 7.3), a more elegant and efficient algorithm for computing contact regions (Sections 8.2 and 8.3), a discussion of algorithm complexity (Section 9), and a variety of more sophisticated examples than in our previous work (Section 10). Possibly most interesting is the new algorithm for computing contact regions, which allows contact point selection to be formulated as a feature detection problem and opens up the possibility of using vision or other sensing to locate good contact points when object geometry is not known.

3. Background

Grasp synthesis, defined as finding a set of contact points on a given object geometry, can be achieved either through optimization or using a constructive algorithm. When optimization techniques are used, the search space is the space of positions of N contacts on an object surface for some N. Optimization criteria vary. For example, Li and Sastry (1987) optimize

Fig. 1. Many typical grasps take advantage of extended areas of contact between the hand and object. Abstracting these grasps as sets of point contacts would require a large number of contacts.

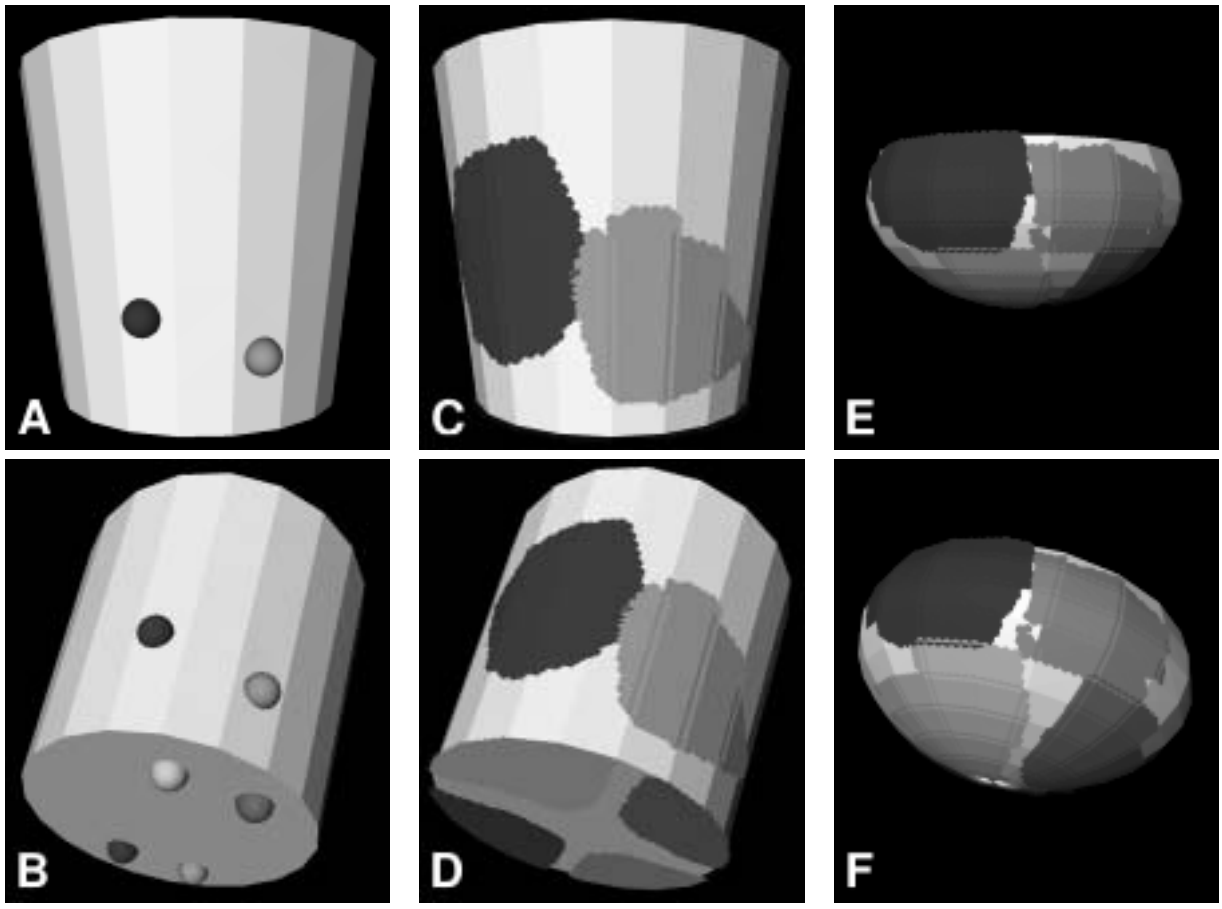

Fig. 2. Our algorithm converts an example grasp into an equivalence class of grasps that can be projected onto any object geometry. (A), (B) An example with eight hard-finger contacts and a friction coefficient of 1.0. (Contacts on the opposite side mirror those shown.) (C), (D) Results for the basket based on this example. The task is to support the object against gravity, and the resulting grasps are “90% as good as the example”, as defined in Section 4. (E), (F) Results for the bowl, based on the same example and quality requirement.

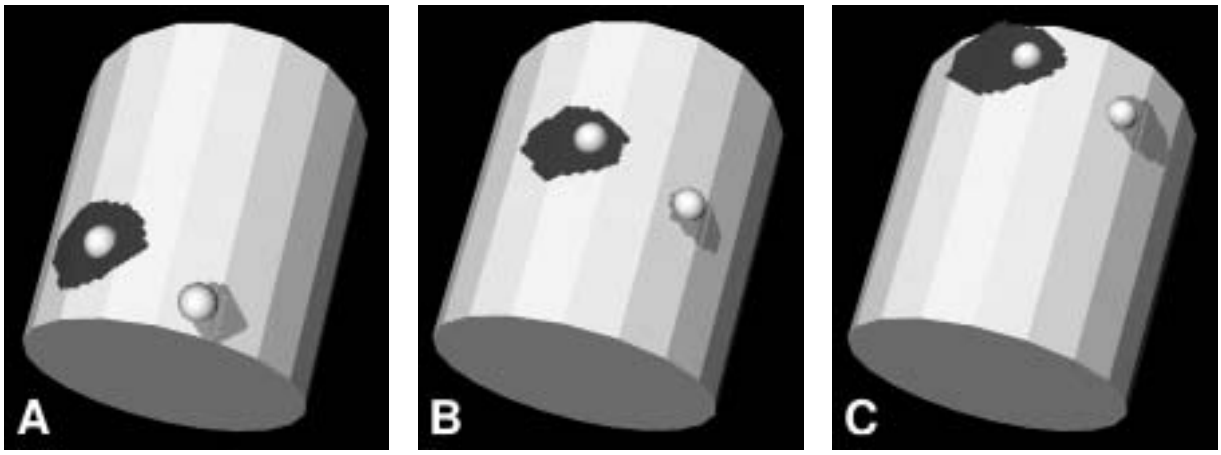

Fig. 3. An example grasp defines the roles of the contacts, and contact regions are constructed around the example. This figure shows how results for a four-contact grasp vary as the contact location of the examples changes. In each figure, contacts on the opposite side mirror those shown, and the contact model, coefficient of friction, and task are the same as those for Figure 2. As in Figure 2, each grasp family represents grasps that are at least 90% as good as the example used to define that family.

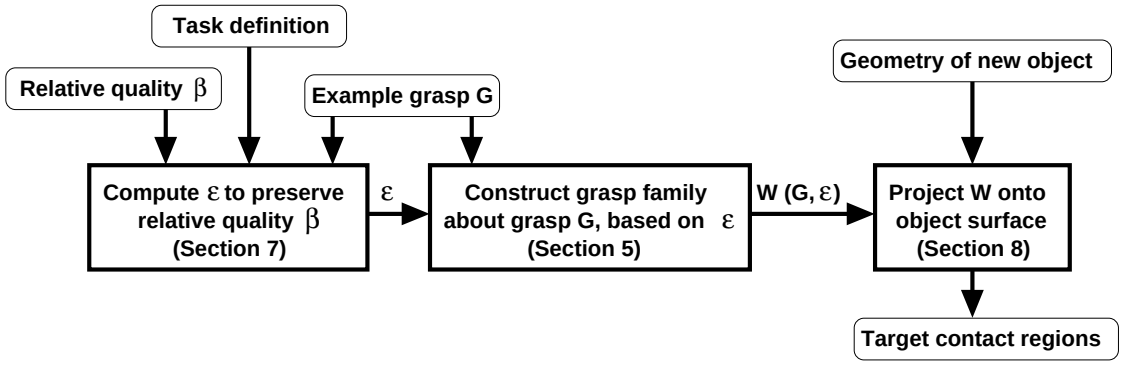

Fig. 4. Block diagram of our grasp synthesis algorithm.

a task-dependent quality measure, where task requirements are described with ellipsoids in force/torque space; Markenscoff and Papadimitriou (1989) minimize compressive forces required to support a polygon against gravity, assumed to act out-of-plane; Mantriota (1999) minimizes the friction coefficient required for a grasp. Zhu, Ding, and Li (2001) and Zhu and Wang (2003) optimize for tasks described as convex polytopes in force/torque space. Lin, Burdick, and Rimon (2000) maximize stiffness of a compliant grasp. Mirtich and Canny (1994) describe algorithms for finding optimal grasps efficiently for two- and three-finger grasps.

In work closest to ours, Ponce, Stam, and Faverjon (1993), Ponce and Faverjon (1995), Ponce et al. (1997), and Chen and Burdick (1993) describe algorithms for optimizing the sizes of independent contact regions for two-to-four-fingered grasps. Van der Stappen, Wentink, and Overmars (2000), Liu (2000), and Li, Yu, and Tsujio (2002) describe a variety of techniques to compute all force-closure grasps for two-dimensional (2D) grasps. Optimal independent contact regions could be extracted from the results of their algorithms using the approach described in Ponce et al. (1997).

Early constructive algorithms for grasp synthesis are due to Nguyen (1988), who presents algorithms to synthesize grasps with two to four fingers. Mishra, Schwartz, and Sharir (1987) point out that, for almost any object with a piecewise smooth surface, force/torque vectors corresponding to frictionless contact at all points on the object surface positively span $\mathbb{R}^6$, which is sufficient to guarantee force-closure. The

trick then is to filter the set of possible contacts down to a small set that also has this property. In their paper, Mishra, Schwartz, and Sharir show that for polyhedra with F triangular faces, an $(F + 6)$-contact frictionless force-closure grasp can always be constructed and iteratively pruned to a force-closure grasp with not more than 12 contacts. Other constructive approaches appear in the area of non-prehensile manipulation (e.g., Mason 1986; Peshkin and Sanderson 1988; Trinkle and Paul 1990; Donald, Jennings, and Rus 1997; Erdmann 1998; Akella and Mason 1998; Lynch and Mason 1999; Zhang and Goldberg 2002) where a sequence of partial force-closure "grasps", possibly with sliding contacts, is used to reconfigure an object.

Our paper is focused on grasps with many contacts. We define many-contact grasps as those with more than the minimum number of contacts required for force-closure. For force-closure in three dimensions with hard-finger contacts, a minimum of seven frictionless contacts are required (Markenscoff, Ni, and Papadimitriou 1990); fewer than seven force/torque vectors cannot positively span $\mathbb{R}^6$. For hard-finger contacts with friction, a minimum of three contacts are always required; with two such contacts, moments about the axis connecting contact points cannot be resisted. Some objects require a minimum of four hard-finger contacts with friction, and four are always sufficient (Markenscoff, Ni, and Papadimitriou 1990). For us, then, many-contact grasps are those having eight or more frictionless contacts or five or more contacts with friction.

Most constructive grasp synthesis algorithms focus on grasps with a minimal number of contacts, or, in the case of Mishra, Schwartz, and Sharir (1987), the number of contacts at which their algorithm terminates, which may often be a true minimum. It is not clear how to extend these algorithms to many-contact grasps except in the trivial case where an acceptable grasp with the minimum number of contacts is constructed and additional contacts are added afterward.

In contrast, optimization approaches can often be extended easily to many-contact grasps. However, the optimization takes place in a space exponential in the number of contacts; each contact can be placed anywhere on an object surface. Many optimization approaches involve placing N contacts on N planar surfaces. Here, optimization may involve nonlinear equations (e.g., Markenscoff and Papadimitriou 1989) or an exponential number of constraints (e.g., Ponce et al. 1997). Zhu, Ding, and Li (2001) point out that if the task is described as a convex polytope in force/torque space, the problem of finding a single best grasp can be expressed as a linear optimization problem in $O(N)$ variables. A suitable set of N planar surfaces must also be selected, however, and the number of combinations from which to choose is exponential in N.

Our paper contributes a constructive technique for grasp synthesis that works for any number of contacts and has running time polynomial in the number of contacts. Our paper builds on the ideas of Ponce et al. (1997) and others to synthesize independent contact regions. In contrast to previous work, however, we make use of an example grasp and construct results that preserve closure properties of that example. This use of an example makes a polynomial time algorithm possible. Our grasps are not in general optimal, but they can be constructed to meet user-specified quality bounds.

In our work, we assume that contact position targets are an appropriate end goal of a grasp synthesis process. An alternative view to generating contact targets is to generate a strategy that will capture or cage the object (Trinkle, Abel, and Paul 1988; Harada and Kaneko 1998; Kaneko, Hino, and Tsuji 1997; Rimon and Blake 1999; Gopalakrishnan and Goldberg 2002).

A number of researchers, motivated by observation of human grasping behavior, have explored the use of grasp taxonomies and behavior-based systems for grasping (Cutkosky and Howe 1990; Bekey et al. 1993; Iberall 1997). One difficulty with such systems is to understand when a given grasping behavior will work and to tune it for a specific object geometry. To address this problem, Kang and Ikeuchi (1994, 1995) present a procedural algorithm for adapting an observed human grasp to the different kinematics of a robot hand. Our algorithm provides an alternative and more general solution; it can be used in conjunction with a behavior-based approach to provide contact targets as regions that guarantee a high-quality grasp can be formed.

Two issues we ignore in this paper are second-order effects and the kinematics of the mechanism that will grasp the object. Force-closure is a first-order effect and our algorithms do not consider local curvature. Second-order analysis can provide insight into the stability of the grasp with respect to external perturbations (e.g., Rimon and Burdick 1998a, 1998b). The kinematics of the mechanism actually determine whether force-closure and other properties of a grasp are achievable (Bicchi 1995). Although this issue is extremely important, it is outside the scope of this paper. We do argue, however, that constructing a space of grasps around a successful example may help to ensure that contact positions and required contact forces on similar objects are achievable simply because the kinematic configuration of the mechanism will be similar in the two grasps. For example, if the objects in Figure 2 are approximately the same size as the basket in the photograph, a robot hand with capabilities similar to the human hand should be able to both reach and apply appropriate forces in the contact areas shown.

An overview of grasping research, including work in grasp synthesis, can be found in Bicchi (2000).

4. Grasp and Force-Closure Preliminaries

In this section we present definitions for grasps, tasks, force-closure, and grasp quality that are used in this paper.

Definitions for terms introduced in this and other sections are provided in the nomenclature.

DEFINITION 1. A **grasp** is a set of contacts.

DEFINITION 2. A **contact** is a location on an object surface, along with information about contact type and local surface properties as required to compute the space of wrenches that can be applied to the object at that location.

We assume that the space of wrenches available at a contact c can be approximated as a linear combination of L extremes and we define $Y(c)$ as the $6 \times L$ matrix of those extremes:

$$Y(c) = \left[\hat{\mathbf{w}}_1(c)\hat{\mathbf{w}}_2(c)\ldots\hat{\mathbf{w}}_L(c)\right] \tag{1}$$

where $\hat{\mathbf{w}}_l(c)$ is normalized so that its component of force normal to the surface is equal to 1. A valid unit wrench $\hat{\mathbf{w}}$ at c can be expressed as a linear combination of extremes where coefficients sum to 1:

$$\hat{\mathbf{w}} = Y(c)\alpha \qquad \alpha \geq \mathbf{0}, \qquad ||\alpha||_{L_1} = 1. \tag{2}$$

This linear model can be used for frictionless point contacts, hard-finger contacts with friction, soft-finger contacts, and any other contact model where the set of available wrenches is convex.

For many tasks, a force-closure grasp is desired.

DEFINITION 3. **Force-closure** is the ability to resist any external wrench with positive forces at the contacts.

We state one proposition that we will use (see, for example, Mishra, Schwartz, and Sharir 1987).

PROPOSITION 1. A grasp can achieve force-closure if and only if the wrench space origin is in the interior of the convex hull of the set of contact wrenches available from the grasp.

We define a task as follows.

DEFINITION 4. A **task** is a set of wrenches that must be applied to the grasped object.

The set of wrenches that make up a task may be designed to obtain a desired outcome such as turning a screwdriver, and it may also include an additional set of wrenches to make the grasp more robust to uncertainty and able to resist external disturbances.

The definition of grasp quality used in this paper is as follows.

DEFINITION 5. **Grasp quality** is the reciprocal of the sum of magnitudes of contact normal forces required to achieve the worst case wrench in a task set.

This definition of grasp quality is based on the notion that the "effort" required for a grasp is related to the sum of magnitudes of contact normal forces as expressed, for example, in Kirkpatrick, Mishra, and Yap (1990), Li and Sastry (1987), and Zhu, Ding, and Li (2001). As a specific illustration of this idea, we compare the quality of the grasps in Figures 2 and 3. The quality of the example grasp in Figure 2 is 0.99, meaning that the sum of magnitudes of contact normal forces to support a 1 kg object is (1/0.99) N = 1.01 N.[1] The grasps in Figures 3(A)–(C) do not have points of support on the bottom surface of the object, and their quality measures are lower: 0.55, 0.48, and 0.29 respectively. The lowest quality grasp is that of Figure 3(C). In this grasp, the contact points are far from the object center of mass, which is near the base of the basket. Here, the sum of magnitudes of contact normal forces required to support a 1 kg object is (1/0.29) N = 3.4 N, more than three times that of the example in Figure 2.

5. Constructing Families of Grasps from a Single Example

This paper explores an approach for generating families of grasps from a single example. As a simple illustration of the idea, consider the problem of planning a three-fingered frictionless grasp of a disk in two dimensions (Figure 5). Only pure forces can be applied to this object with frictionless contacts; no torques can be generated about the object center of mass. An equilibrium grasp of the disk can be formed from a set of contacts if the forces at those contacts positively span $\mathbb{R}^2$. Suppose we wish to create a collection of contact regions such that placing each contact anywhere in its region guarantees this property. In the absence of any other requirements, these regions can be made equal in size and evenly distributed. One such set of regions is shown in Figure 5. Most of the resulting grasps are not optimal, but they do meet the given design goal.

The regions in Figure 5 were constructed by selecting a set of three evenly distributed forces to fix the coordinate frame and growing regions around this example to be as large as possible while still guaranteeing that any triple of forces formed from the regions would positively span $\mathbb{R}^2$. This construction can be done in time polynomial in the number of contacts, and any number of contacts can be accommodated. Figure 6 shows similar constructions for four- and five-contact grasps of a frictionless disk. For clarity, a single region is highlighted in each case. Figure 6 shows that one advantage of having more contacts is increased flexibility in contact placement. This flexibility can help to accommodate variability in object geometry and constraints due to kinematics of a robot hand.

The process implied in Figures 5 and 6 can be extended to the full six-dimensional (6D) wrench space and made to work for any given example grasp such as that shown in the left column of Figure 2. The remainder of this section describes our technique for creating a family of grasps from a single example, adapted from Pollard (1996) and Pollard and Hodgins (2002). For reference, Figure 7 provides a 2D illustration of the construction process.

1. The result is not exactly 1 N in part because we allow for some variation in object orientation (see the description of the gravity task in Section 10).

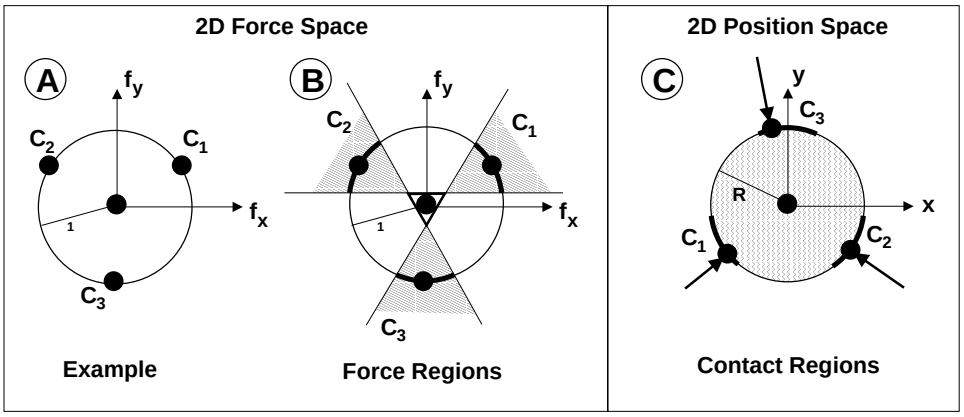

Fig. 5. Equally sized, evenly distributed, independent contact regions for a three contact grasp. (A) Example with evenly distributed contact points. (B) Regions in a 2D force space. (C) Regions in a 2D position space. Selecting one contact force within each region in B or one contact point within each region in (C) guarantees that forces span $\mathbb{R}^2$ and an equilibrium grasp can be formed. One possible equilibrium grasp is shown in (C).

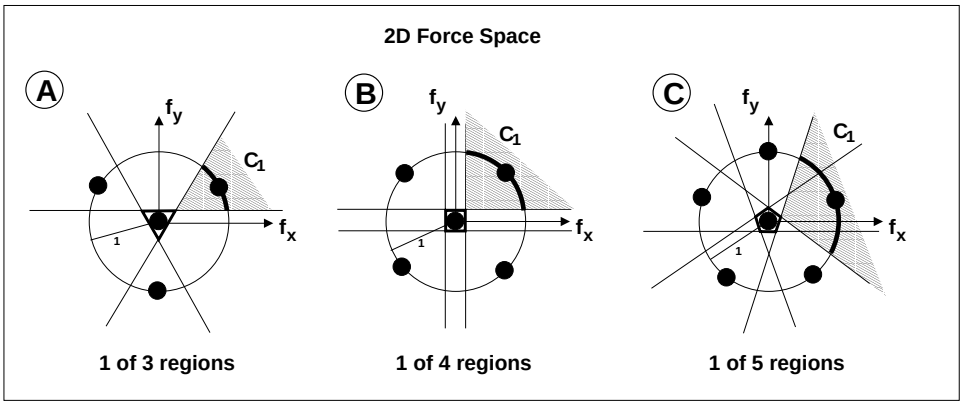

Fig. 6. Construction geometry for equally sized, evenly distributed contact regions for three-, four-, and five-contact grasps. Only one region is highlighted in each case. Region size, along with flexibility in placing contact points, grows with the number of contacts in a grasp.

Suppose we are given an example grasp G having N contacts $g_1, \ldots, g_N$. Wrenches available at each contact are represented as a linear combination of L extremes. The example, then, can be represented as the collection of NL extreme wrenches $\hat{\mathbf{w}}_l(g_n)$:

$$G = \left\{\hat{\mathbf{w}}_1(g_1), \ldots, \hat{\mathbf{w}}_L(g_N)\right\}. \tag{3}$$

We assume that the $\hat{\mathbf{w}}_l(g_n)$ span $\mathbb{R}^6$, although they may not positively span $\mathbb{R}^6$.

The construction process begins with a volume in $\mathbb{R}^6$, the convex hull of all of the $\hat{\mathbf{w}}_l(g_n)$. This volume is significant because it captures the closure properties of G and is a first step in constructing many force-based quality measures. We will represent this volume, CH_{orig}, as a collection of half-spaces, each expressed as an outward pointing normal $\hat{\mathbf{n}}_h$ and a distance from the wrench space origin d_h.[2]

2. Although the $\hat{\mathbf{w}}_l(g_n)$ are physical quantities, i.e., force/torque vectors, for the purposes of this construction they are considered to be points in a 6D Euclidean space. The first three dimensions are the force vector, normalized to have magnitude 1, and the last three dimensions are the torque vector. We make this switch from the space of wrenches to $\mathbb{R}^6$ to develop a definition of grasp families preserving closure properties of the example, and in Section 8 we describe how these results are then mapped back to physically achievable wrenches for a given object. Because the $\hat{\mathbf{w}}_l(g_n)$ are considered to be points in $\mathbb{R}^6$, constructing CH_{orig} is meaningful, half-space normals $\hat{\mathbf{n}}_h$ have unit magnitude using the L_2 norm in $\mathbb{R}^6$, and we will use the standard inner product in $\mathbb{R}^6$ (e.g., $(\hat{\mathbf{w}} \cdot \hat{\mathbf{n}}) = \sum_{i=1}^{6} w_i n_i$). Although treating a wrench as a point in $\mathbb{R}^6$ may seem questionable because torque directions are compared directly to force directions, our results are not affected by this assumption; they rely on comparing capabilities of a new grasp to those of an example, and the outcome of this comparison does not change with choice of wrench space origin or with unit of measure of distance.

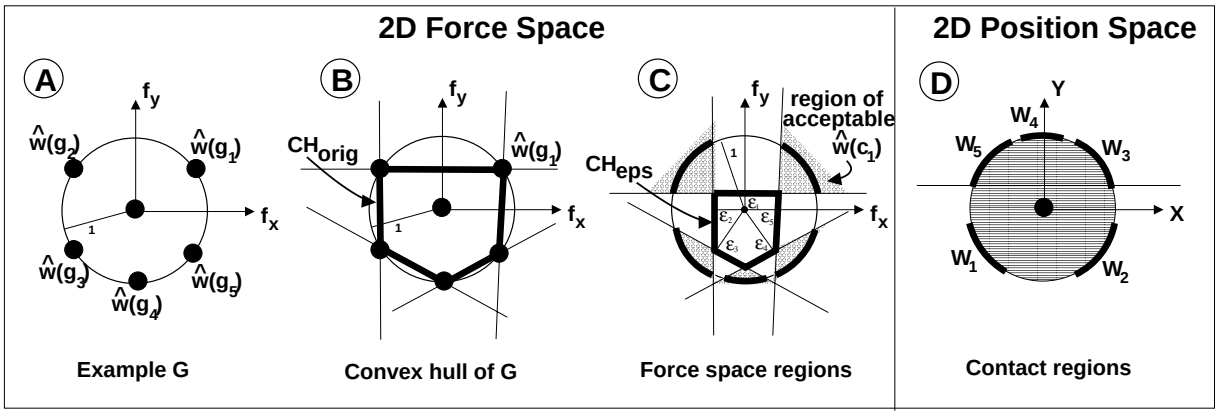

Fig. 7. A 2D example construction of regions $W_n(G, \epsilon)$. (A) A frictionless example grasp G consisting of five contact wrenches. (B) CH_{orig} is the convex hull of these contact wrenches. Half-space boundaries are also shown. (C) CH_{eps} is constructed from CH_{orig} by moving each half-space boundary h to distance ϵ_h from the origin. The region of acceptable wrenches $\hat{\mathbf{w}}(c_n)$ is an intersection of exterior half-spaces of CH_{eps}. (D) Each such region can be mapped to a set of contact points on an object (Section 8) to obtain target contact regions $W_n(G, \epsilon)$. Grasps in the family $W(G, \epsilon)$ have one contact in each of these regions.

$$CH_{orig}(G) = \{\begin{bmatrix} \hat{\mathbf{n}}_1 \\ d_1 \end{bmatrix}, \begin{bmatrix} \hat{\mathbf{n}}_2 \\ d_2 \end{bmatrix}, \ldots, \begin{bmatrix} \hat{\mathbf{n}}_H \\ d_H \end{bmatrix}\} \\ = \textit{ConvexHull(G)}. \tag{4}$$

To represent the connection between half-space boundaries in CH_{orig} and wrenches $\hat{\mathbf{w}}_l(g_n)$, we define index set $\rho_{n,l}$ so that $h \in \rho_{n,l}$ implies that the half-space boundary h passes through point $\hat{\mathbf{w}}_l(g_n)$.

$$\rho_{n,l}(G) = \{h : (\hat{\mathbf{w}}_l(g_n) \cdot \hat{\mathbf{n}}_h) = d_h\}. \tag{5}$$

For each half-space h, we choose some ϵ_h to reflect the requirements of the task. Choosing $\epsilon_h = d_h$ will match capabilities of the example grasp, but if the example is unnecessarily strong in certain directions, setting ϵ_h to a value less than d_h will allow greater flexibility in contact placement. Details on setting ϵ_h can be found in Section 7.

Let $\epsilon = [\epsilon_1 \ldots \epsilon_H]$. Based on $CH_{orig}(G)$, $\rho_{n,l}(G)$, and task variables ϵ, we define an equivalence class of grasps $W(G, \epsilon)$ as a set of regions $W_n(G, \epsilon)$, one for each contact, as follows:

$$W(G, \epsilon) = \{c_1, \ldots, c_N : c_n \in W_n(G, \epsilon), \quad n = 1, \ldots, N\} \tag{6}$$

$$W_n(G, \epsilon) = \bigcap_{l=1}^{L} W_{n,l}(G, \epsilon) \tag{7}$$

$$W_{n,l}(G, \epsilon) = \left\{c_n : \exists \alpha_l \text{ s.t. } \left((Y(c_n)\alpha_l) \cdot \hat{\mathbf{n}}_h \geq \epsilon_h\right) \right. \\ \left. \forall h \in \rho_{n,l}, \quad \alpha_l \geq \mathbf{0}, \quad ||\alpha_l||_{L_1} = 1\right\}. \tag{8}$$

For any grasp in the set W, contact c_n is meant to correspond directly to the contact g_n in G. In other words, the role of contact c_n is defined by the set of wrenches $\hat{\mathbf{w}}_1(g_n), \ldots, \hat{\mathbf{w}}_L(g_n)$ from the example grasp. The valid region for contact c_n is constructed as the intersection of L regions $W_{n,l}$, one for each wrench extreme $\hat{\mathbf{w}}_l(g_n), l = 1, \ldots, L$. Region $W_{n,l}$ is based on the intersection of exterior half-spaces associated with $\hat{\mathbf{w}}_l(g_n)$ (i.e. half-spaces indexed by $\rho_{n,l}$) after those half-spaces have been adjusted along their normals to distances ϵ_h; some unit wrench available at contact c_n must fall within this intersection. Sections 6 and 7 show how this particular definition makes it possible to control closure and quality properties of all grasps in $W(G, \epsilon)$.

In the frictionless case, $L = 1$ and subscript l is not needed, resulting in the following expression for contact region W_n, which is much cleaner and is illustrated in Figure 7(D):

$$W_n(G, \epsilon) = \left\{c_n : \hat{\mathbf{w}}(c_n) \cdot \hat{\mathbf{n}}_h \geq \epsilon_h \qquad \forall h \in \rho_n\right\} \\ \textit{(frictionless case only)}. \tag{9}$$

6. Properties of Grasps in a Given Family

Given the construction technique in Section 5, what can we say about grasps in W? The main result of the paper is the following proposition.

PROPOSITION 2. Suppose we are given grasp C having contacts $\{c_1, \ldots, c_N\}$ and grasp family $W(G, \epsilon)$ constructed as in eq. (6).

From eq. (4), $CH_{orig}(G)$ is the convex hull of the unit wrench extremes of G:

$$\begin{aligned} CH_{orig}(G) = & \ ConvexHull\{\hat{\mathbf{w}}_1(g_1), \ldots, \hat{\mathbf{w}}_L(g_N)\} \\ & = \left([\hat{\mathbf{n}}_1 d_1]^{\mathrm{T}}, \ldots, [\hat{\mathbf{n}}_H d_H]^{\mathrm{T}}\right). \end{aligned} \tag{10}$$

We define $CH_{new}(C)$ as the convex hull of the unit wrench extremes of C:

$$CH_{new}(C) = \ ConvexHull\left\{\hat{\mathbf{w}}_1(c_1), \ldots, \hat{\mathbf{w}}_L(c_N)\right\}. \tag{11}$$

Let $CH_{eps}(G, \epsilon)$ be the intersection of all half-spaces having normals $\hat{\mathbf{n}}_h$ and distances ϵ_h:

$$CH_{eps}(G, \epsilon) = \{[\hat{\mathbf{n}}_1 \epsilon_1]^{\mathrm{T}}, \ldots, [\hat{\mathbf{n}}_H \epsilon_H]^{\mathrm{T}}\}. \tag{12}$$

Then, if grasp C is in grasp family $W(G, \epsilon)$, $CH_{new}(C)$ contains $CH_{eps}(G, \epsilon)$:

$$\boxed{C \in W(G, \epsilon) \longrightarrow CH_{new}(C) \supseteq CH_{eps}(G, \epsilon).} \tag{13}$$

A proof sketch can be found in Appendix A. This proposition describes the volume $CH_{eps}(G, \epsilon)$ in $\mathbb{R}^6$ (possibly empty) that is contained within the convex hull of contact wrenches of any grasp in the family $W(G, \epsilon)$. This volume is shown for a 2D example in Figure 7(C).

7. Meeting Design Goals

Because CH_{eps} in eq. (12) is determined by the values of ϵ_h, properties of grasps in $W(G, \epsilon)$ can be controlled through careful selection of these parameters.

7.1. Force-Closure

By Proposition 1, grasps in W will be force-closure if the convex hull of the contact wrenches available from any grasp in W contains the origin in its interior. By Proposition 2, it is sufficient that CH_{eps} in eq. (12) contain the origin in its interior. This goal is achieved by setting the following constraint:

$$\boxed{\epsilon_h > 0 \qquad h = 1, \ldots, H.} \tag{14}$$

Any small number can be used for all ϵ_h to ensure that force-closure is possible for all grasps in $W(G, \epsilon)$.

7.2. Grasp Quality

A force-closure grasp is not necessarily a desirable grasp, as it may result in large internal forces to counter small external wrenches. Referring to Definition 4, suppose we are given a task T described as the convex hull of K points $\mathbf{s}_k$: $T = ConvexHull(\mathbf{s}_1, \ldots, \mathbf{s}_K)$. For this task, by Definition 5, the quality of the example grasp is

$$Q(G) = \min_{h=1}^{H} \left(\frac{d_h}{\max(\mathbf{0}, \max_{k=1}^{K}(\mathbf{s}_k \cdot \hat{\mathbf{n}}_h))} \right) \tag{15}$$

(see also Zhu and Wang 2003).

To obtain new grasps with quality at least $\beta Q(G)$, we set ϵ_h as follows:

$$\boxed{\epsilon_h = \beta Q(G) \max\left(\mathbf{0}, \max_{k=1}^{K}(\mathbf{s}_k \cdot \hat{\mathbf{n}}_h)\right) \quad h = 1, \ldots, H.} \tag{16}$$

Using Proposition 2, we can show easily that $C \in W(G, \epsilon)$ and eq. (16) imply that

$$Q(C) \geq \beta Q(G). \tag{17}$$

Now suppose the task is not known. We note that eqs. (15) and (16) imply that $\epsilon_h \leq \beta d_h$ for any task T. As a result, we can also obtain grasps with quality at least $\beta Q(G)$ by setting

$$\boxed{\epsilon_h = \beta d_h \qquad h = 1, \ldots, H.} \tag{18}$$

Equation 18 is intriguing because it shows that contact forces can be bounded relative to an example without measuring those forces and without knowing anything about the task. However, using eq. (16) when the task is known may result in larger contact target regions corresponding to directions where the example grasp is unnecessarily strong.

7.3. Partial Force-Closure Grasps

The construction techniques presented in the paragraphs above can also be used when the example is not force-closure, but instead has the property of partial force-closure over a wrench set G' (Bicchi 1995). For synthesis of partial force-closure grasps, we make use of the following variation of Proposition 2.

LEMMA 1. Suppose we are given grasp C' having contacts $\{c_1, \ldots, c_M\}$ and grasp family $W(G', \epsilon)$ constructed as in eq. (6), except with $CH_{orig}(G')$ also containing the zero wrench:

$$\begin{aligned} CH_{orig}(G') = & \ ConvexHull\{\hat{\mathbf{w}}_1(g_1), \ldots, \hat{\mathbf{w}}_L(g_M), \mathbf{0}\} \\ & = \{[\hat{\mathbf{n}}_1 d_1]^{\mathrm{T}}, \ldots, [\hat{\mathbf{n}}_H d_H]^{\mathrm{T}}\}. \end{aligned} \tag{19}$$

We define $CH_{new}(C')$ as the convex hull of the unit wrench extremes of C' and the zero wrench:

$$CH_{new}(C') = \ ConvexHull\left\{\hat{\mathbf{w}}_1(c_1), \ldots, \hat{\mathbf{w}}_L(c_M), \mathbf{0}\right\}. \tag{20}$$

Let $CH_{eps}(G', \epsilon)$ be the intersection of all half-spaces having normals $\hat{\mathbf{n}}_h$ and distances ϵ_h:

$$CH_{eps}(G', \epsilon) = \{[\hat{\mathbf{n}}_1 \epsilon_1]^{\mathrm{T}}, \ldots, [\hat{\mathbf{n}}_H \epsilon_H]^{\mathrm{T}}\}. \tag{21}$$

Let

$$\rho_{zero} = \{h : d_h = 0\}. \tag{22}$$

Suppose

$$\epsilon_h = 0 \qquad \forall h \in \rho_{zero}. \tag{23}$$

Then, if grasp $C^{'}$ is in grasp family $W(G^{'}, \epsilon)$, $CH_{new}(C^{'})$ contains $CH_{eps}(G^{'}, \epsilon)$:

$$C^{'} \in W(G^{'}, \epsilon) \longrightarrow CH_{new}(C^{'}) \supseteq CH_{eps}(G^{'}, \epsilon). \tag{24}$$

Proof sketch. From $G^{'}$, we create an example $G = \{\hat{\mathbf{w}}_1(g_1), \ldots, \hat{\mathbf{w}}_L(g_M), \mathbf{0}, \ldots, \mathbf{0}\}$ with $\mathbf{0}$ repeated L times, to be used in Proposition 2. Matching this Lemma to Proposition 2, we have $N = M + 1$, and $CH_{orig}(G) = CH_{orig}(G^{'})$. Because all facets containing $\hat{\mathbf{w}}_l(g_N) = \mathbf{0}$ pass through the origin, we know that index set $\rho_{N,l}$ points only to half-space boundaries containing the origin, or

$$d_h = 0 \qquad \forall h \in \rho_{N,l}, \tag{25}$$

which implies that $\rho_{N,l} \subseteq \rho_{zero}$. Given eq. (23), ϵ_h can be replaced with $\mathbf{0}$ in the expression for $W_{N,l}$:

$$W_{N,l}(G^{'}, \epsilon) = \left\{c_N : \exists \alpha_l \text{ s.t. } \left((Y(c_N)\alpha_l) \cdot \hat{\mathbf{n}}_h \geq \mathbf{0}\right) \forall h \in \rho_{N,l}, \right.$$
$$\left. \alpha_l \geq \mathbf{0}, ||\alpha_l||_{L_1} = 1\right\}. \tag{26}$$

It follows that $\mathbf{0}$ is an acceptable substitute for all of the wrenches $Y(c_N)\alpha_l = \hat{\mathbf{w}}_l(c_N)$, which implies in turn that $CH_{new}(C^{'})$ is an acceptable substitute for $CH_{new}(C)$. By Proposition 2, then, $CH_{new}(C^{'})$ contains $CH_{eps}(G, \epsilon)$. Because $CH_{orig}(G) = CH_{orig}(G^{'})$, it is also true that $CH_{eps}(G, \epsilon) = CH_{eps}(G^{'}, \epsilon)$. It follows that $CH_{new}(C^{'})$ contains $CH_{eps}(G^{'}, \epsilon)$, completing the proof. □

Using the construction in Lemma 1, we can generate grasps having partial force-closure over the same wrench set as the example by using

$$\epsilon_h = 0 \quad \forall h \in \rho_{zero} \qquad \epsilon_h > 0 \quad \forall h \notin \rho_{zero}. \tag{27}$$

Arbitrary tasks can be handled by setting ϵ_h as in eq. (16) as long as

$$\max\left(0, \max_{k=1}^{K}(\mathbf{s}_k \cdot \hat{\mathbf{n}}_h)\right) = 0 \qquad \forall h \in \rho_{zero}. \tag{28}$$

Equation 28 states that the task must have zero component in any direction in which the example cannot apply wrenches; in other words, the example must be capable of achieving the task.

Situations where the task is unknown can be handled by setting $\epsilon_h = \beta d_h$ as described in eq. (18). Parameter d_h is zero for $h \in \rho_{zero}$ by definition, preserving the requirement of eq. (23).

8. Incorporating Object Geometry

Grasp family $W(G, \epsilon)$ (eq. (6)) is expressed in a manner independent of object geometry. The equation

$$W(G, \epsilon) = \{c_1, \ldots, c_N : c_i \in W_n, \quad n = 1, \ldots, N\} \tag{29}$$

describes all possible combinations of contacts that can be generated from a given example using our construction technique. This section describes three ways to filter such a set of grasps through an object's geometry: (1) sample the object surface and test contact points for inclusion in W_n; (2) map constraints bounding W_n onto planar patches of an object surface; (3) map constraints bounding W_n into three-dimensional (3D) Cartesian space.

8.1. Sampling the Object Surface and Testing for Inclusion in W_n

With any object, even one with a complex curved surface, a sample and test approach can be used to identify contact regions. This technique was used for the examples shown in Figure 2. The entire object surface is sampled, and each sample point is tested for inclusion in $W_n(G, \epsilon)$, $n = 1, \ldots, N$. Given contact c_n, and with reference to eq. (8), the problem of determining whether $c_n \in W_n$ can be specified as follows:

$$\text{find } Lx1 \text{ vector of coefficients } \alpha_l \text{ and parameter } \nu_{n,l} \text{ to maximize } \nu_{n,l} \text{ such that} \tag{30}$$

$$(Y(c_n)\alpha_l) \cdot \hat{\mathbf{n}}_h \geq \epsilon_h \nu_{n,l} \qquad \forall h \in \rho_{n,l} \tag{31}$$

$$\alpha_l \geq \mathbf{0} \tag{32}$$

$$||\alpha_l||_{L_1} = 1. \tag{33}$$

Then from eq. (7):

$$c_n \in W_n \Longleftrightarrow \left(\min_{l=1}^{L} \nu_{n,l}\right) \geq 1. \tag{34}$$

This problem description states that there must be some unit contact wrench available at c_n (i.e., some valid value for α_l) such that all half-space constraints are met or exceeded by this wrench (i.e., $\nu_{n,l} \geq 1$ for all $l = 1, \ldots L$).

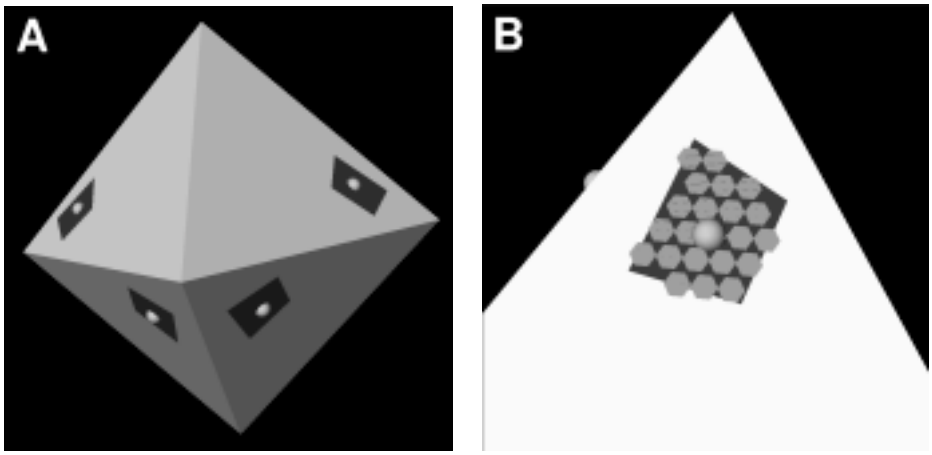

Fig. 8. (A) Contact regions for an eight-contact frictionless grasp of an octahedron. Example contact points are shown as spheres. The back view of contact points and regions is identical to the front view, and grasps shown are guaranteed to be capable of achieving force-closure (eq. (14)). (B) Sampling versus 2D mapping comparison in the frictionless case. The two algorithms produce the same results when there is no friction.

In the frictionless case, $c_n \in W_n$ can be determined more easily. From eq. (9) and Figure 7:

$$c_n \in W_n \Longleftrightarrow \hat{\mathbf{w}}(c_n) \cdot \mathbf{n}_h \geq \epsilon_h \qquad \forall h \in \rho_n. \tag{35}$$

In this case, at each sample point on the frictionless surface the contact wrench $\hat{\mathbf{w}}(c_n)$ is formed and tested for inclusion in W_n by checking just a few 6D dot products.

Figure 8 shows results for an eight-contact grasp of an octahedron when contacts are frictionless. Figure 9 shows results for the octahedron using the same example grasp, but with coefficient of friction set to 0.5.

8.2. Mapping Constraints Bounding W_n onto an Object Surface

If the object consists of planar surfaces, a mapping algorithm can be used to find contact regions on each surface. This algorithm is perhaps more elegant than the sample-and-test approach of Section 8.1 because it avoids a brute force sampling of the surface. It will obtain contact regions more quickly than a sample-and-test approach if the object is composed of large planar faces.

The basic idea is to project the 6D half-space constraints that define $W_n(G, \epsilon)$ directly onto the planar surface, avoiding the need to sample that surface as in Section 8.1. Referring to eq. (8), region $W_{n,l}$ consists of a collection of half-space constraints in the form $(\hat{\mathbf{w}}(c_n) \cdot \hat{\mathbf{n}}_h) \geq \epsilon_h$. If $\hat{\mathbf{w}}(c_n)$ were a linear function of position on a planar surface, then these half-space constraints could be projected easily onto the surface, and their intersection would form a patch on that surface.

The difficulty is that a non-trivial contact model does not have a single wrench $\hat{\mathbf{w}}(c_n)$ available at a given contact point. Wrench $\hat{\mathbf{w}}(c_n)$ can be any linear combination of basis wrenches $Y(c_n)\alpha_l$ where $\alpha_l \geq \mathbf{0}$ and $||\alpha_l||_{L_1} = 1$.

Our solution is to sample this space of wrenches and accumulate results over the set of samples. Suppose we take J samples of the space of wrenches available at a given contact. Each sample $\hat{\mathbf{w}}_j(c_n)$ can be parametrized by its location (u, v) on the surface patch. The force component of $\hat{\mathbf{w}}_j(c_n)$ does not depend on u or v, and the torque component varies linearly with u and v, and so $\hat{\mathbf{w}}_j(c_n)$ can be written as

$$\hat{\mathbf{w}}_j(c_n) = \hat{\mathbf{w}}_j(u, v) = \mathbf{w}_{j,0} + u\mathbf{w}_{j,u} + v\mathbf{w}_{j,v}. \tag{36}$$

Given eq. (36), each half-space constraint $\hat{\mathbf{w}}_j(c_n) \cdot \hat{\mathbf{n}}_h \geq \epsilon_h$ can be projected onto the 2D surface to obtain:

$$(\hat{\mathbf{w}}_{j,0} \cdot \hat{\mathbf{n}}_h) + u(\hat{\mathbf{w}}_{j,u} \cdot \hat{\mathbf{n}}_h) + v(\hat{\mathbf{w}}_{j,v} \cdot \hat{\mathbf{n}}_h) \geq \epsilon_h. \tag{37}$$

We call this projection $P_j([\hat{\mathbf{n}}_h d_h]^{\mathrm{T}})$.

For a single sample j, the projection of $W_{n,l}$ onto the planar surface is the intersection of results for all active constraints $h \in \rho_{n,l}$ (eq. (8)). We take the union of results over all J samples. Linear combinations of samples are also acceptable, and so we take the convex hull of this result. We call this patch $P(W_{n,l})$:

$$P(W_{n,l}) = \mathit{ConvexHull}\left(\bigcup_{j=1}^{J}\left(\bigcap_{h\in\rho_{n,l}} P_j([\hat{\mathbf{n}}_h d_h]^{\mathrm{T}})\right)\right). \tag{38}$$

From eq. (7), we take the intersection over all l friction cone extremes to get the final patch for contact n, defined by region W_n:

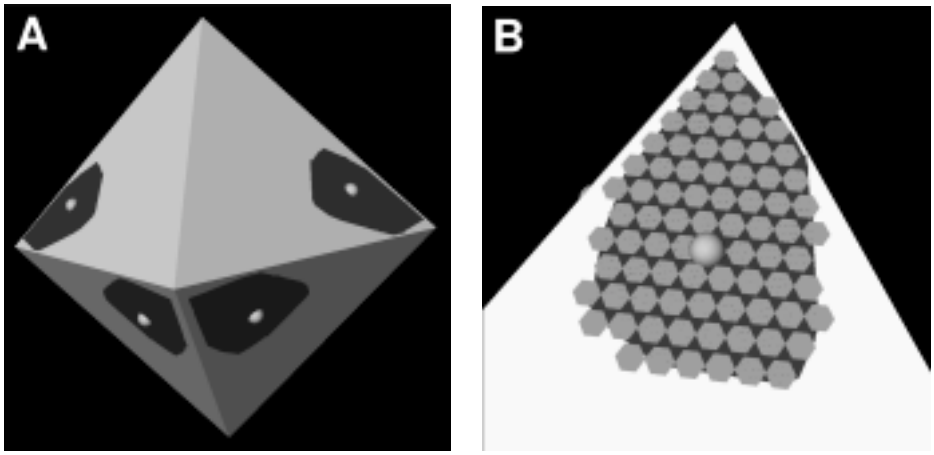

Fig. 9. (A) Contact regions for an eight-contact grasp with friction. Example contact points are shown as spheres. The back view of contact points and regions is identical to the front view shown. The coefficient of friction is 0.5, the task is a unit ball in wrench space, and grasps shown are guaranteed to be at least 40% as good as the example. (B) Sampling versus 2D mapping comparison in the case with friction. The 2D mapping is a conservative approximation when there is friction.

$$P(W_n) = \bigcap_{l=1}^{L} ConvexHull\left(\bigcup_{j=1}^{J}\left(\bigcap_{h\in\rho_{n,l}} P_j([\hat{\mathbf{n}}_h d_h]^{\mathrm{T}})\right)\right). \tag{39}$$

Figures 8 and 9 show comparisons between sample and 2D mapping results for hard-finger contact without and with friction, respectively. Sample points are shown as hexagons, and the 2D mapping results are shown as a solid colored region beneath the hexagons.

In the case with friction, the mapping computed using this approach is conservative for two reasons. First, the friction cone is approximated as a friction pyramid. The sample and test approach of Section 8.1 also uses this approximation. Secondly, a contact point on the planar surface may meet all constraints for region W_n and yet not be captured by $P(W_n)$. This is because the intersection of the projections of two half-space constraints onto a planar surface follows a non-linear path on the surface when contact wrenches are linearly interpolated between two extremes $\hat{\mathbf{w}}_{j_1}(c_n)$ and $\hat{\mathbf{w}}_{j_2}(c_n)$. Equation 39 makes a linear approximation of this path with the convex hull operation. This approximation is conservative, and it is typically quite good, as can be seen by comparing the sampling and projection approaches in Figure 9. It becomes worse when the friction cone is large, when the number of samples is very sparse, or when the surface normal of the new object is far from that of the example grasp. In all cases, results can be made as good as desired by adding more wrench space samples j to the union operation in eq. (39), including samples in the interior. (Our results used six samples on the boundary of the friction cone.)

8.3. Mapping Constraints Bounding W_n into Cartesian Space

An interesting and very simple variation on mapping contact region W_n onto a planar surface is to map this contact region into 3D space. Given an expected surface normal $\hat{\mathbf{f}}$, sample wrenches can be written as a linear function of world coordinates (x, y, z). Half-space constraints can then be projected into 3D space in a manner analogous to eq. (37), resulting in

$$(\hat{\mathbf{w}}_{j,0}\cdot\hat{\mathbf{n}}_h) + x(\hat{\mathbf{w}}_{j,x}\cdot\hat{\mathbf{n}}_h) + y(\hat{\mathbf{w}}_{j,y}\cdot\hat{\mathbf{n}}_h) + z(\hat{\mathbf{w}}_{j,z}\cdot\hat{\mathbf{n}}_h) \geq \epsilon_h. \tag{40}$$

We call this projection $P_{j,3D}([\hat{\mathbf{n}}_h d_h]^{\mathrm{T}})$. Contact region n, defined by W_n, can then be expressed as

$$P_{3D}(W_n) = \bigcap_{l=1}^{L} ConvexHull\left\{\bigcup_{j=1}^{J}\left[\bigcap_{h\in\rho_{n,l}} P_{j,3D}\left([\hat{\mathbf{n}}_h d_h]^{\mathrm{T}}\right)\right]\right\}. \tag{41}$$

In the frictionless case, $P_{3D}(W_n)$ is the infinite extrusion along $\hat{\mathbf{f}}$ of the 2D surface projection $P(W_n)$ for any planar surface with the same normal. This result reflects the fact that a frictionless contact wrench does not change as the surface moves in the direction of its normal. If results for a range of surface normals $\hat{\mathbf{f}}$ are intersected or if there is a more complex contact model, projection $P_{3D}(W_n)$ will be finite.

A projection of contact region W_n into 3D space is useful when object geometry is not known in detail. Given an estimate of object center of mass, eq. (41) describes where in space to look for a geometric feature having surface normal $\hat{\mathbf{f}}$.

Table 1. Algorithm Complexity for N Contacts, L Wrench Extremes in the Contact Model, J Wrench Samples in the Contact Model (Possibly Including Interior Samples), H Half-Spaces in CH_{orig}, K Wrench Extremes in the Task Model, S Samples on the Object Surface, and F Planar Faces in the Object Surface

Current paper	Compute ϵ	$O((NL)^4 + HK)$ (including computing CH_{orig})
	Compute $W(G, \epsilon)$	Constant time (if CH_{orig} is available)
	Compute regions (sampling)	$O(NLS)$ linear optimization problems in $O(L)$ variables
	Compute regions (projection)	$O(FN(LJH \log(LJH)))$
Zhu, Ding, and Li (2001)	Complete algorithm	$O(F^N)$ linear optimization problems in $O(NLK)$ variables

9. Computational Complexity

Referring to Figure 4, the grasp synthesis algorithm has three parts: (1) compute parameter ϵ; (2) compute grasp family $W(G, \epsilon)$; (3) map W onto the surface of a new object to obtain contact regions. Here we show that all parts are polynomial in the number of contacts N (Table 1) and we compare the complexity of this algorithm with the elegant competing technique of Zhu, Ding, and Li (2001).

Computing ϵ is trivial unless we are preserving a force-based quality value as in Section 7.2. In this case, the convex hull $CH_{orig}(G)$ must be computed to obtain parameters d_h and $\hat{\mathbf{n}}_h$ in eqs. (15) and (16). Computing $CH_{orig}(G)$ requires time $O((NL)^4)$ for the giftwrapping algorithm in six dimensions (Preparata and Shamos 1985) with N the number of contacts and L the number of samples in the contact model. Given a task represented with K wrench extremes, time $O(HK)$ is also required to set values for ϵ_h once CH_{orig} has been computed (eqs. (15) and (16)). Family $W(G, \epsilon)$ is constructed as part of the computation of CH_{orig} and requires no additional computation time.

To map W onto an object surface, the sample and test approach in Section 8.1 requires solving $O(NLS)$ linear optimization problems, where S is the number of samples taken of the object surface. (See eqs. (30)–(34).) Each linear optimization problem has $L + 1$ variables; the simplex algorithm theoretically requires time exponential in L (but not N), and in practice is much faster.

To map W onto an object surface using the projection approach in Section 8.2 requires computation time $O(FN(LJH \log(LJH)))$. Given F planar faces on the object, each of these must be tested for inclusion in all N regions W_n. The various intersection and union operations performed on the 2D facet require time proportional to $a \log a$, where $a = LJH$. The LJH term derives from the maximum of H half-space constraints that must be projected onto the surface, the union over J samples and intersection over L samples (eq. (39)). All operations on the planar facet are either convex hull construction or half-space intersection, resulting in the log term in the expression $LJH \log(LJH)$.

We compare this result to the algorithm presented in Zhu, Ding, and Li (2001). The algorithm in Zhu, Ding, and Li (2001) is suitable for finding either a single optimal grasp or a set of grasps exceeding a quality measure similar to that described in Section 7.2. To find a globally optimal solution, the algorithm in Zhu, Ding, and Li (2001) requires solving $O(F^N)$ linear optimization problems in $(NLK+1)$ variables. The $O(F^N)$ term arises because all combinations of N faces (F choose N) must be tested to guarantee that a solution is globally optimal.

Practically, when the object has few faces F, the algorithm in Zhu, Ding, and Li (2001) may be faster than that presented here. For an eight-contact grasp of an octahedron, for example, our algorithm requires computing a 6D convex hull and then projecting each target contact region onto the eight planar faces. The complete running time for our implementation is 50 s on a 1.6 GHz machine.[3] In contrast, for this same problem, if we know that there must be one contact on each of the eight planar faces, the algorithm in Zhu, Ding, and Li (2001) would require solving a single linear optimization problem in 193 variables.[4]

As the number of faces increases, however, our algorithm will scale much more gracefully than that in Zhu, Ding, and Li (2001), or any other global optimization approach that requires finding the best set of N planar faces. For example, the bowl in Figure 2 has 820 faces. For this problem and with the same parameters as the octahedron example, our algorithm requires 11 min to compute contact target regions. However, for the algorithm in Zhu, Ding, and Li (2001), the complexity of selecting the best N faces results in an unwieldy solution; 5×10^{18} (820 choose eight) combinations of faces must either be examined or somehow discarded in searching for a globally optimal solution. For objects with smooth surfaces, the authors suggest that a local search technique may be more effective (Zhu and Wang 2003), although they also show that such an approach is, of course, subject to the problem of local minima, and results depend on the starting point of the search.

Like the approach of Zhu, Ding, and Li (2001), our approach is a global one, and it considers the entire surface of the object. The primary advantage of our approach is that com-

3. This example assumed eight hard-finger contacts with friction ($N = 8$). It used a friction pyramid approximation with six extremes ($L = 6$) and a task approximation with four extremes ($K = 4$).

4. The number of variables is $NLK + 1$, with $N = 8$, $L = 6$, and $K = 4$.

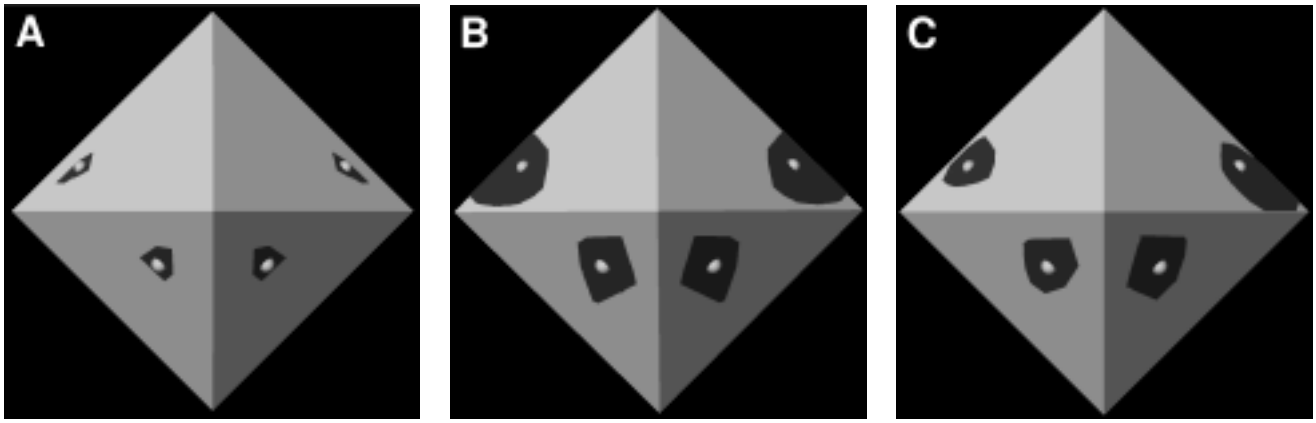

Fig. 10. Effect of task variation in the eight-contact grasp of the octahedron. The regions on the back of the object are reflections of the regions on the front about a plane parallel to the image plane and passing through the object center of mass. The contact model is hard-finger contact with coefficient of friction 0.5, and grasps shown are guaranteed to be at least 80% as good as the example. (A) Wrench space ball task. (B) Gravity task. (C) Rotation task.

putation time is polynomial in the number of contacts, with computation time growing more gracefully with the number of contacts and complexity of the object surface. What makes our polynomial time algorithm possible is the availability of an example grasp and the decision to produce not a single optimal grasp, but a set of grasps that are similar to the example and exceed a given quality measure. In cases where an appropriate example is available from experience or observation, our approach may be more practically useful for constructing grasps having many contacts.

10. Results

One of the main features of the algorithm presented in this paper is the ability to meet a variety of task goals. As an example of this capability, Figures 10 and 11 show contact regions for three different tasks: (1) the wrench space ball task, where nothing is assumed to be known about the directions of task wrenches; (2) the gravity task, represented as a range of force vectors within an angle of 20° about vertical; (3) a rotation task such as pouring, represented as the force vectors for the gravity task, swept through a 90° rotation from vertical to horizontal.

In general, regions become larger in directions that are not important for a task. For the rotation task, the octahedron is tipped to the left in the view shown, and the mug is tipped so that the handle rotates upward. The value of the desired relative quality measure determines region size, as illustrated in Figure 12 for the wrench space ball task.

Forming an acceptable grasp with many contacts is easier in some ways than forming a grasp with a minimal number of contacts, in the sense that contact region size will grow with the number of contacts. In fact, if there is a very large number of contacts, randomly placing them on the object surface may often produce a good grasp. Figure 13 compares our use of the contact regions to random contact placement. Results are for the five-contact grasp of the mug and the rotation task. The plot on the left shows the distribution of the quality measure (Definition 5) for randomly generated grasps for two cases. In the first case (solid line), grasps were generated by selecting one point randomly within each contact region. In the second case (dashed line), grasps were generated by placing each point randomly on the object surface. The plot on the right shows the fraction of all samples exceeding quality measures ranging from 0 to 1.4. In the first case (solid line), the lower bound for the contact regions was quality 0.6, and all grasps that were generated with one contact point in each region exceed this bound. In the second case (dashed line), quality measures range from zero to 1.3, and 15% of grasps do not have a non-negative quality measure, indicating that they are not adequate to perform the rotation task. On the other hand, it is interesting to note that more than 30% of the time, the randomly generated grasps do exceed the quality measure specified for this task. Of course, the distributions of contacts produced by these grasps will not in general be similar to the example and may be unacceptable for reasons not captured by this quality metric.

In Section 7.3 we described how non-force-closure grasps could be handled. Neither the gravity nor the rotation task require force-closure grasps. Thus, we can form contact regions for these tasks even when the example grasp is not force-closure. Figure 14 shows results for a 12-contact frictionless grasp of the octahedron and the gravity task. When there is no friction, the example grasp is clearly not force-closure, as pure forces in the upward direction cannot be resisted.

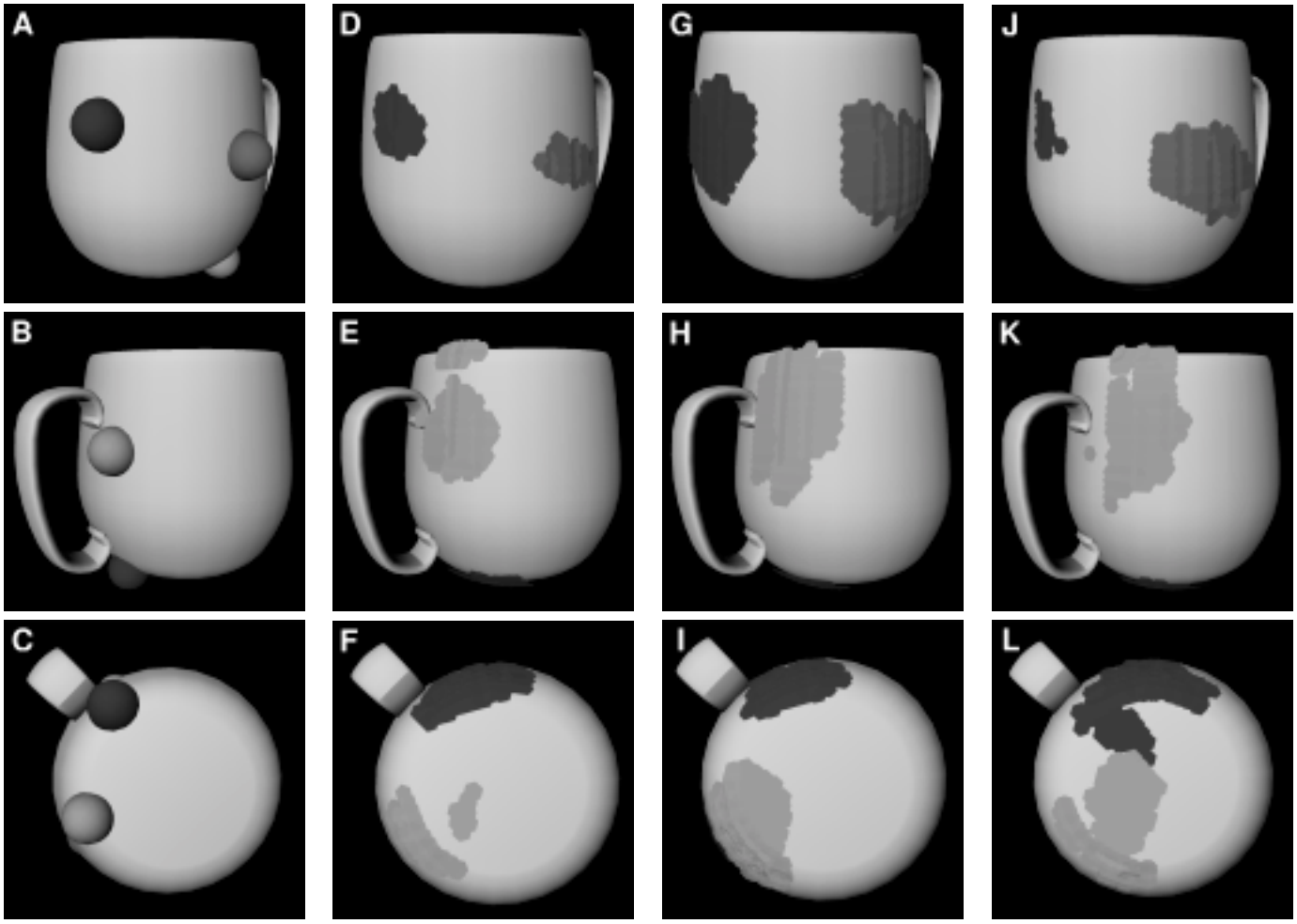

Fig. 11. Effect of task variation on a five-contact grasp of a mug. The contact model is hard-finger contacts with coefficient of friction 1.0. (A), (B), (C) Example grasp. (D), (E), (F) Regions for the wrench space ball task, with grasps guaranteed at least 80% as good as the example. (G), (H), (I) Regions for the gravity task, with grasps guaranteed at least 80% as good as the example. (J), (K), (L) Regions for the rotation task, with grasps guaranteed at least 115% as good as the example.

We used early versions of this approach to plan grasps for a robot hand and to create manipulation plans from a human demonstration for a humanoid robot (Figure 15). In both cases we take advantage of the ability to adapt examples to new geometries; the example grasp and manipulation plan are obtained from objects that are geometrically simpler than the ultimate target objects. Details of these experiments are given in Pollard (1996) and Pollard and Hodgins (2002), respectively.

11. Discussion

In this paper we have shown that a family of grasps can be derived from an example and expressed as a set of independent contact regions. The focus of the paper is on grasps having a relatively large number of contacts. Advantages of this construction technique are computational efficiency, flexibility in contact placement, and ability to preserve closure and quality properties of an example grasp. In exchange for these advantages, we give up optimality. This technique does not in general produce minimal force grasps, or maximal contact regions. However, a space of grasps can be constructed that exceed a user-specified measure of grasp quality.

For constructions that preserve grasp quality (Section 7.2), we have assumed that the sum of magnitudes of contact normal forces represents grasp effort. However, in most circumstances all contacts are not equivalent. For example, contact on the distal link of a finger will typically be weaker than contact at a more proximal link. One trivial extension to our algorithm is to assign a weight to each contact to obtain a more accurate measure of grasp effort. A more thorough extension

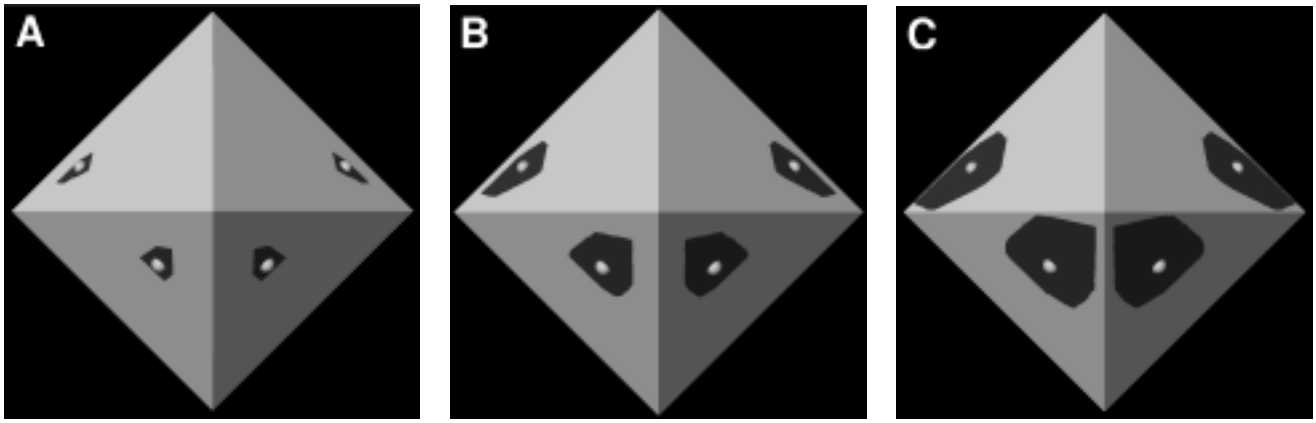

Fig. 12. Effect of quality variation in the eight-contact grasp of the octahedron. The view from the opposite side of the object is identical. The contact model is hard-finger contact with coefficient of friction 0.5, and regions are shown for the wrench space ball task. Grasps guaranteed at least (A) 80%, (B) 60%, and (C) 40% as good as the example.

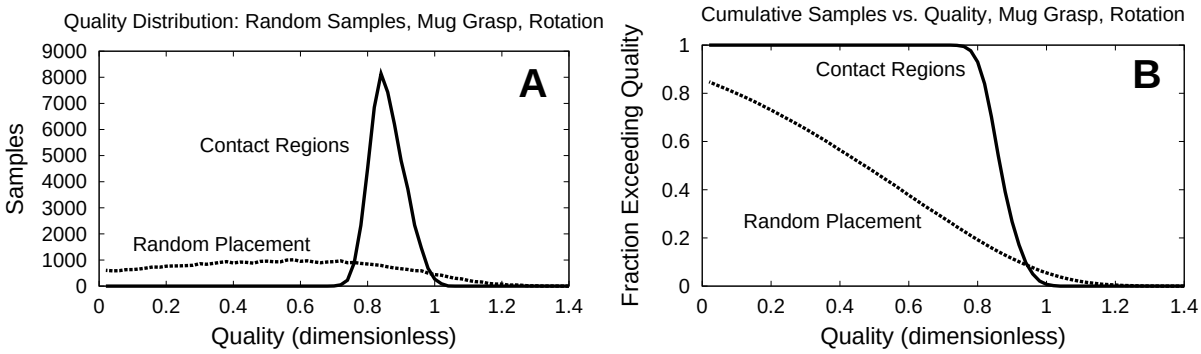

Fig. 13. (A) Distribution of quality values. Five-contact grasps of the mug are randomly generated by placing one contact in each region (solid line) or by placing each contact randomly on the object surface (dashed line). (B) Percentage of samples with quality exceeding values ranging from 0 to 1.4.

would better take into account finger kinematics, including coupling between contacts on a single finger and the relative independence of different fingers. This is one topic of future work.

Our results depend on the choice of example. For the mug, for instance, the example is a good one for supporting the object against gravity ($Q(G) = 1.11$), and large regions are obtained for a quality measure $Q(C) \geq 0.8Q(G) \geq 0.89$. The example is a poor one for the wrench space ball task, however ($Q(G) = 0.022$), and even with the very small quality measure $Q(C) \geq 0.8Q(G) \geq 0.018$, where contact forces may be more than 50 times the magnitude of some task wrench, regions obtained are small.

The dependence of results on the example raises the question of how to create a good one. Can an example be chosen automatically? The best example may be one that results in large contact targets for a given object geometry and task. Alternatively, we may wish for a single example to provide large contact targets for a class of objects. The observation that grasps can be classified into relatively few types (e.g. Cutkosky and Howe 1990) suggests that a small library of examples may be sufficient. Finding good examples automatically is another topic of future research.

The idea of processing an example to find contact geometry targets in Cartesian space was only touched upon in this paper. We are also investigating the possibility of developing suites of feature detectors that can be used both to choose contact points and to select between examples when object geometry is not known but features can be sensed.

To move toward a more practical use of these results, we would like to revisit the reach-to-grasp problem given a set of contact target regions and investigate techniques for control-

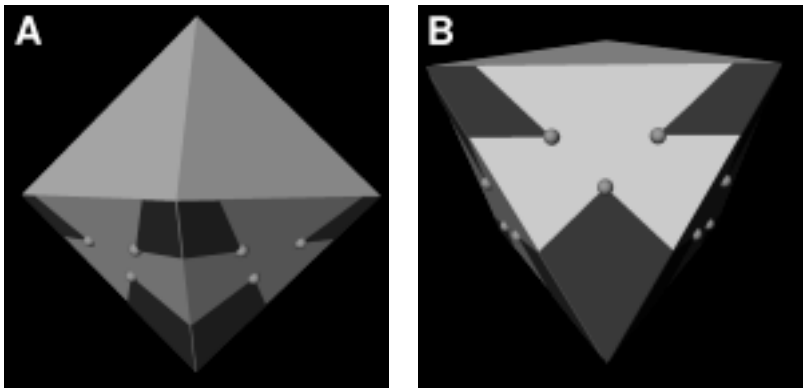

Fig. 14. 12-contact frictionless grasp of the octahedron with the gravity task. (A) View of entire grasp. (B) Close-up of one face. Contacts are placed at the same locations on each of the four lower faces. The example grasp is not force-closure, and grasps generated with one contact in each region are not force-closure, but they are adequate for supporting the object against gravity.

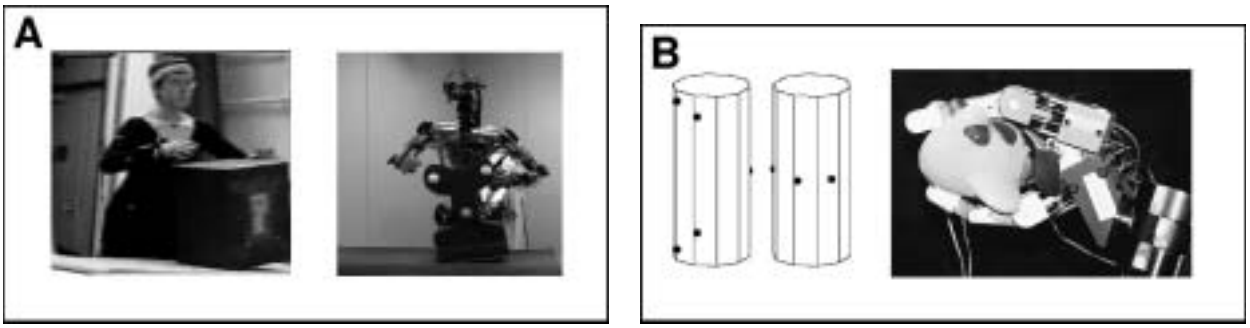

Fig. 15. (A) The plan for manipulating this object was adapted from motion capture of a person manipulating a box of similar size. (B) This grasp of the airplane was identified based on an example seven-contact grasp of a cylinder. In both cases, the creation of target contact regions from the example (as opposed to finding a unique optimal grasp) was important for accommodating the kinematic constraints of the robot.

ling task forces once the object has been grasped. Of particular interest are situations that are dynamic (as in Chevallier and Payandeh 1997) or where there is a large amount of uncertainty. Having examples of successful grasp and manipulation strategies may make possible interesting new approaches in these areas as well.

Appendix A

Sketch of proof for Proposition 2. Given a new grasp $C \in W(G, \epsilon)$, suppose $CH_{new}(C)$ does not contain $CH_{eps}(G, \epsilon)$. Choose some point $\mathbf{p}$ in CH_{eps} that lies outside CH_{new}. Choose some hyperplane F bounding CH_{new} that does not contain $\mathbf{p}$ in its interior. Let the half-space constraint represented by F be $[\hat{\mathbf{n}} d]^{\mathrm{T}}$. Based on this constraint and our assumptions, the following are true:

$$\mathbf{q} \cdot \hat{\mathbf{n}} \leq d \qquad \forall \mathbf{q} \in CH_{new} \tag{42}$$

$$\hat{\mathbf{w}}_l(c_n) \cdot \hat{\mathbf{n}} \leq d \qquad l = 1, \ldots, L, \quad n = 1, \ldots, N \tag{43}$$

$$\mathbf{p} \cdot \hat{\mathbf{n}} > d. \tag{44}$$

These equations state respectively that all points $\mathbf{q}$ of CH_{new} are contained within the given half-space, all wrench extremes of grasp C, $\hat{\mathbf{w}}_l(c_n)$, are contained within the given half-space (because they are contained in $CH_{new}(C)$), and point $\mathbf{p}$ is not contained within the given half-space.

Find a vertex $\hat{\mathbf{w}} = \hat{\mathbf{w}}_i(g_j)$ in $CH_{orig}(G, \epsilon)$ that maximizes $\hat{\mathbf{w}} \cdot \hat{\mathbf{n}}$. Assume CH_{orig} has only simplicial facets (true if $\hat{\mathbf{w}}_l(g_n)$ are in general position). There will be at least six facets of CH_{orig} containing $\hat{\mathbf{w}}$. Choose any six of them so that their normals span $\mathbb{R}^6$.[5] Denote these six facets with index set $\rho'_{j,i} \subseteq$

5. There will always be at least one such set, because CH_{orig} is not degenerate; we assume the set of $\hat{\mathbf{w}}_l(g_n)$ spans $\mathbb{R}^6$ (Section 5).

$\rho_{j,i}$. Compute $\hat{\mathbf{w}}'$ so that

$$\hat{\mathbf{w}}' \cdot \hat{\mathbf{n}}_h = \epsilon_h \qquad \forall h \in \rho'_{j,i}. \tag{45}$$

Wrench $\hat{\mathbf{w}}'$ is the intersection of the hyperplanes bounding the six half-spaces $[\hat{\mathbf{n}}_h \epsilon_h]^{\mathrm{T}}$ for h in $\rho'_{j,i}$.

PROPOSITION 3. No portion of CH_{eps} lies beyond $\hat{\mathbf{w}}'$ in the $\hat{\mathbf{n}}$ direction.

Proof sketch. We know that

$$\hat{\mathbf{n}}_h \cdot \hat{\mathbf{n}} \geq 0 \qquad \forall h \in \rho'_{j,i}. \tag{46}$$

Otherwise, $\hat{\mathbf{w}}'$ would not be the extreme on CH_{orig} that is the greatest distance in the $\hat{\mathbf{n}}$ direction. It follows that the intersection of interior half-spaces $[\hat{\mathbf{n}}_h \epsilon_h]^{\mathrm{T}}$ for $h \in \rho'_{j,i}$ is a convex cone with apex at $\hat{\mathbf{w}}'$ and pointing away from $\hat{\mathbf{n}}$. However, half-space constraints $[\hat{\mathbf{n}}_h \epsilon_h]^{\mathrm{T}}$ bound CH_{eps}, and all of CH_{eps} must fall within this cone. Therefore, no portion of CH_{eps} lies beyond $\hat{\mathbf{w}}'$ in the $\hat{\mathbf{n}}$ direction, completing the proof of Proposition 3. □

Because $\hat{\mathbf{w}}'$ is an extreme of CH_{eps} in the $\hat{\mathbf{n}}$ direction (Proposition 3), $\mathbf{p} \in CH_{eps}$ (by definition), and with reference to eq. (44), we can state that

$$(\hat{\mathbf{w}}' \cdot \hat{\mathbf{n}}) \geq (\mathbf{p} \cdot \hat{\mathbf{n}}) > d. \tag{47}$$

Because contact c_j of the new grasp is contained in region W_j, it is also contained within $W_{j,i}$, and eq. (8) implies that

$$\begin{aligned} &\exists \alpha_i \text{ s.t. } \left((Y(c_j)\alpha_i) \cdot \hat{\mathbf{n}}_h \geq \epsilon_h\right) \forall h \in \rho'_{j,i}, \quad \alpha_i \geq \mathbf{0}, \\ &\quad ||\alpha_i||_{L_1} = 1. \end{aligned} \tag{48}$$

Let $\hat{\mathbf{w}}_{c_j} = Y(c_j)\alpha_i$ for some valid value of α_i.

PROPOSITION 4. $\hat{\mathbf{w}}_{c_j}$ is contained within $CH_{new}(C)$.

Proof sketch. $Y(c_j)$ is defined as the set of unit wrenches available at contact c_j. By definition of $CH_{new}(C) = ConvexHull(C) = ConvexHull\{\hat{\mathbf{w}}_1(c_1), \ldots, \hat{\mathbf{w}}_1(c_j), \ldots, \hat{\mathbf{w}}_L(c_j), \ldots, \hat{\mathbf{w}}_L(c_N)\}$, all basis wrenches of $Y(c_j)$ are contained in $CH_{new}(C)$. By constraints on α_i in eq. (48), $\hat{\mathbf{w}}_{c_j}$ lies in the convex hull of $\hat{\mathbf{w}}_l(c_j)$ and so it is also contained in $CH_{new}(C)$. □

Now from eq. (48) and the definition of $\hat{\mathbf{w}}_{c_j}$

$$\left(\hat{\mathbf{w}}_{c_j} \cdot \hat{\mathbf{n}}_h \geq \epsilon_h\right) \qquad \forall h \in \rho'_{j,i}. \tag{49}$$

Because $\hat{\mathbf{n}}_h \cdot \hat{\mathbf{n}} \geq 0$ for all h in $\rho'_{j,i}$ (eq. (46)), eq. (49) states that contact wrench $\hat{\mathbf{w}}_{c_j}$ is contained in a convex cone based at $\hat{\mathbf{w}}'$ and pointing in the direction of $\hat{\mathbf{n}}$. The closest such wrench within this cone and in the $\hat{\mathbf{n}}$ direction is $\hat{\mathbf{w}}'$ and so

$$(\hat{\mathbf{w}}_{c_j} \cdot \hat{\mathbf{n}}) \geq (\hat{\mathbf{w}}' \cdot \hat{\mathbf{n}}) \geq (\mathbf{p} \cdot \hat{\mathbf{n}}) > d, \tag{50}$$

implying that $\hat{\mathbf{w}}_{c_j}$ is beyond facet $[\hat{\mathbf{n}} d]^{\mathrm{T}}$ and so it is not contained in $CH_{new}(C)$. This contradiction with Proposition 4 completes the proof. □

Acknowledgments

The author would like to thank Mike Erdmann, Alon Wolf, and the anonymous reviewers for many helpful comments on this paper, Mitsuo Kawato and Gordon Cheng for hosting productive visits to ATR in Japan, Jessica Hodgins for assistance with human motion capture experiments, and Darrin Bentivegna for much assistance with the robot experiments. This research was supported in part by National Science Foundation (NSF) CAREER award CCR-0093072, and NSF grants ECS-0325383, ECS-0326095, and ANI-0224419.

References

Akella, S. and Mason, M. T. 1998. Posing polygonal objects in the plane by pushing. *International Journal of Robotics Research* 17(1):70–88.

Bekey, G. A., Liu, H., Tomovic, R., and Karplus, W. J. 1993. Knowledge-based control of grasping in robot hands using heuristics from human motor skills. *IEEE Transactions on Robotics and Automation* 9(6):709–722.

Bicchi, A. 1995. On the closure properties of robotic grasping. *International Journal of Robotics Research* 14(4):319–334.

Bicchi, A. 2000. Hands for dexterous manipulation and robust grasping: A difficult road toward simplicity. *IEEE Transactions on Robotics and Automation* 16(6):652–662.

Chen, I.-M. and Burdick, J. W. 1993. Finding antipodal point grasps on irregularly shaped objects. *IEEE Transactions on Robotics and Automation* 9(4):507–512.

Chevallier, D. P. and Payandeh, S. 1997. On computation of grasping forces in dynamic manipulation using a three-fingered grasp. *Journal of Mechanisms and Machine Theory* 33(3):225–244.

Cutkosky, M. R. and Howe, R. D. 1990. Human grasp choice and robot grasp analysis. *Dextrous Robot Hands*, S. Venkataraman and T. Iberall, editors, Springer-Verlag, New York.

Donald, B. R., Jennings, J., and Rus, D. 1997. Information invariants for distributed manipulation. *International Journal of Robotics Research* 16(5):673–702.

Erdmann, M. 1998. An exploration of non-prehensile two-palm manipulation. *International Journal of Robotics Research* 17(5):485–503.

Gopalakrishnan, K. and Goldberg, K. 2002. Gripping parts at concave vertices. *Proceedings of the IEEE International Conference on Robotics and Automation*, Washington, DC.

Harada, K. and Kaneko, M. 1998. Enveloping grasp for multiple objects. *Proceedings of the IEEE International Conference on Robotics and Automation*, Leuven, Belgium.

Iberall, T. 1997. Human prehension and dextrous robot hands. *International Journal of Robotics Research* 16(3).

Kaneko, M., Hino, Y., and Tsuji, T. 1997. On three phases for achieving enveloping grasps. *Proceedings of the IEEE*

International Conference on Robotics and Automation, Albuquerque, NM.

Kang, S. B. and Ikeuchi, K. 1994. Robot task programming by human demonstration: mapping human grasps to manipulator grasps. *Proceedings of the IEEE/RSJ International Conference on Intelligent Robots and Systems*, Munich, Germany.

Kang, S. B. and Ikeuchi, K. 1995. Toward automatic robot instruction from perception – temporal segmentation of tasks from human hand motion. *IEEE Transactions on Robotics and Automation* 11(5):670–681.

Kirkpatrick, D. G., Mishra, B., and Yap, C. K. 1990. Quantitative Steinitz's theorems with applications to multifingered grasping. *Proceedings of the 22nd ACM Symposium on Theory of Computing*, Baltimore, MD, May 14–16.

Li, Z., and Sastry, S. 1987. Optimal grasping by multifingered robot hands. *Proceedings of the IEEE International Conference on Robotics and Automation*, Raleigh, NC.

Li, Y., Yu, Y., and Tsujio, S. 2002. An analytical grasp planning on given object with multifingered hand. *Proceedings of the IEEE International Conference on Robotics and Automation*, Washington, DC.

Lin, Q., Burdick, J. W., and Rimon, E. 2000. A stiffness-based quality measure for compliant grasps and fixtures. *IEEE Transactions on Robotics and Automation* 16(6):675–688.

Liu, Y.-H. 2000. Computing n-finger form-closure grasps on polygonal objects. *International Journal of Robotics Research* 19(2):149–158.

Lynch, K. M. and Mason, M. T. 1999. Dynamic nonprehensile manipulation: controllability, planning, and experiments. *International Journal of Robotics Research* 18(1):64–92.

Mantriota, G. 1999. Communication on optimal grip points for contact stability. *International Journal of Robotics Research* 18(5):502–513.

Markenscoff, X. and Papadimitriou, C. H. 1989. Optimum grip of a polygon. *International Journal of Robotics Research* 8(2):17–29.

Markenscoff, X., Ni, L., and Papadimitriou, C. H. 1990. The geometry of grasping. *International Journal of Robotics Research* 9(1):61–74.

Mason, M. T. 1986. Mechanics and planning of manipulator pushing operations. *International Journal of Robotics Research* 5(3):53–71.

Mirtich, B., and Canny, J. 1994. Easily computable optimum grasps in 2-d and 3-d. *Proceedings of the IEEE International Conference on Robotics and Automation*, San Diego, CA.

Mishra, B., Schwartz, J. T., and Sharir, M. 1987. On the existence and synthesis of multifinger positive grips. *Algorithmica* 2(4):541–558.

Nguyen, V. 1988. Constructing force-closure grasps. *International Journal of Robotics Research* 7(3):3–16.

Peshkin, M. A. and Sanderson, A. C. 1988. Planning robotic manipulation strategies for workpieces that slide. *International Journal of Robotics and Automation* 4(5):524–531.

Pollard, N. S. 1996. Synthesizing grasps from generalized prototypes. *Proceedings of the IEEE International Conference on Robotics and Automation*, Minneapolis, MN.

Pollard, N. S. and Hodgins, J. K. 2002. Generalizing demonstrated manipulation tasks. *Workshop on the Algorithmic Foundations of Robotics*, Nice, France.

Ponce, J. and Faverjon, B. 1995. On computing three-finger force-closure grasps of polygonal objects. *IEEE Transactions on Robotics and Automation* 11(6):868–881.

Ponce, J., Stam, D., and Faverjon, B. 1993. On computing force-closure grasps of curved two-dimensional objects. *International Journal of Robotics Research* 12(3):263–273.

Ponce, J., Sullivan, S., Sudsang, A., Boissonnat, J.-D., and Merlet, J.-P. 1997. On computing four-finger equilibrium and force-closure grasps of polyhedral objects. *International Journal of Robotics Research* 16(1):11–35.

Preparata, F. P. and Shamos, M. I. 1985. *Computational Geometry*, Springer-Verlag, New York.

Rimon, E. and Blake, A. 1999. Caging planar bodies by one-parameter two-fingered gripping systems. *International Journal of Robotics Research* 18(3):299–318.

Rimon, E. and Burdick, J. W. 1998a. Mobility of bodies in contact—Part I: a 2nd-order mobility index for multiple-finger grasps. *IEEE Transactions on Robotics and Automation* 14(5):696–708.

Rimon, E. and Burdick, J. W. 1998b. Mobility of bodies in contact—Part II: how forces are generated by curvature effects. *IEEE Transactions on Robotics and Automation* 14(5):709–717.

Trinkle, J. C. and Paul, R. P. 1990. Planning for dexterous manipulation with sliding contacts. *International Journal of Robotics Research* 9(3):24–48.

Trinkle, J. C., Abel, J. M., and Paul, R. P. 1988. An investigation of frictionless enveloping grasping in the plane. *International Journal of Robotics Research* 7(3):33–51.

Van der Stappen, A. F., Wentink, C., and Overmars, M. H. 2000. Computing immobilizing grasps of polygonal parts. *International Journal of Robotics Research* 19(5):467–479.

Zhang, M. T. and Goldberg, K. 2002. Gripper point contacts for part alignment. *IEEE Transactions on Robotics and Automation* 18(6):902–910.

Zhu, X. and Wang, J. 2003. Synthesis of force-closure grasps on 3D objects based on the Q distance. *IEEE Transactions on Robotics and Automation* 19(4):669–679.

Zhu, X., Ding, H., and Li, H. 2001. A quantitative measure for multi-fingered grasps. *Proceedings of the IEEE/ASME International Conference on Advanced Intelligent Mechatronics*, Como, Italy, July 8–12.